A Study on The Heterogeneity of Tropical Cyclone Vulnerability Functions in Different Provinces along The Coastal Areas in China

Chenning Pan
Joint International Research Laboratory of Catastrophe Simulation and Systemic Risk Governance, Beijing Normal University, Zhuhai 519087, China;
School of National Safety and Emergency Management, Beijing Normal University, Zhuhai 519087, China
202321099015@mail.bnu.edu.cn

Xiaoyong Ni*
Joint International Research Laboratory of Catastrophe Simulation and Systemic Risk Governance, Beijing Normal University, Zhuhai 519087, China;
School of National Safety and Emergency Management, Beijing Normal University, Zhuhai 519087, China
nixiaoyong@bnu.edu.cn

Xifan Shen
Bay Area International Business School, Beijing Normal University, Zhuhai 519087, China
202111059036@mail.bnu.edu.cn

Ziyi Peng
Bay Area International Business School, Beijing Normal University, Zhuhai 519087, China
2960830241@qq.com

*Correspondence: nixiaoyong@bnu.edu.cn

ABSTRACT

Coastal regions in China have long been plagued by tropical cyclone (TC) disasters, and TC vulnerability function for disaster-bearing bodies is a widely used quantitative vulnerability assessment method in face of TCs. TC vulnerability functions may vary across different regions due to geographical heterogeneity, hindering this method from universal use. This study systematically collects a 15-year-long dataset from 12 provinces in China. Six alternative TC vulnerability functions are comprehensively investigated by province, and a library of the optimal TC vulnerability functions for three kinds of disaster-bearing bodies, that is, economic, population, and crop in different provinces is developed. The heterogeneity of TC vulnerability in different provinces along the coastal areas in China is then thoroughly analyzed. This paper provides a deeper understanding of the spatial heterogeneity characteristics of disasters and disaster-bearing bodies, and provides good references for local departments to carry out more targeted disaster prevention and reduction work.

Keywords

Tropical cyclone, vulnerability functions, coastal areas in China, disaster loss assessment.

INTRODUCTION

Tropical cyclones (TCs) are low-pressure vortices that occur over tropical or subtropical oceans. A TC with a central sustained wind speed of 32.7 to 41.4 meters per second is named as a typhoon (located in the western North Pacific) or a hurricane (located in other typhoon-prone regions) (WMO, 2022; National Meteorological

Information Center, 2023). It is reported that TCs are natural disasters that have a wide range of impacts and are extremely destructive. Over the past twenty years, there have been a total of about two thousand tropical storms globally with a wide distribution in Asia, North America and Europe. The number of people affected by TCs accounted for 19.52%; the number of deaths and missing persons accounted for 19.17%; and the direct economic losses accounted for 48.57% of the total global natural disasters (Academy of Disaster Reduction and Emergency Management et al., 2023). Relevant data show that the TC disaster is one kind of the main natural disasters faced by human beings, which needs great and urgent attention.

The area of China's coastal provinces and provinces adjacent to coastal provinces is a typical region most severely hit by typhoons (Xu et al., 2015; Wan et al., 2023). Every year, a large number of typhoons make landfall in the southeastern coastal areas of China, causing huge losses. In August 14th, 2019, typhoon "Likima" affected a total of 14.02 million people in China with 2.10 million people urgently relocated, and caused 57 deaths, as well as a direct economic loss of 53.72 billion yuan. In September 5th, 2023, typhoon "Haikui" had caused record-breaking extreme rain in Fujian, Guangdong, and other places. Many findings also suggest that typhoon disasters in coastal areas in China will become increasingly severe in the future (Lee et al., 2020; Wang et al., 2021). Therefore, it is of great significance to study typhoon disasters in China's coastal areas.

In this study, the classic method of typhoon vulnerability functions is utilized to depict the current typhoon risk in China's coastal area. It is widely recognized that typhoon vulnerability functions have significant spatial heterogeneity. This paper currently focuses on the heterogeneity of typhoon vulnerability functions in different provinces along the coastal areas in China. Considering that the loss of typhoon disasters not only depends on the typhoon intensity itself, but also depends on the resilience characteristics of disaster-bearing bodies and the scientific nature of disaster prevention measures, the authors believe that the results provided by this paper have an important reference value for improving emergency management capabilities and strategies in future emergency work in face of typhoons.

The remainder of the paper is organized as follows. Section 2 is the literature review, which reviews the application areas of vulnerability curve methods and their specific applications in typhoon loss assessment. Section 3 outlines the writing approach of the article. Section 4 introduces the research area and data sources used in the paper. Section 5 presents the form of vulnerability curves selected for this study. Section 6 analyzes the heterogeneity of vulnerability curves in the study area. Section 7 discusses the limitations of the research and future directions. Finally, Section 8 summarizes the main findings and their significance.

LITERATURE REVIEW

Vulnerability and Vulnerability Curve

With the concept of "vulnerability" being widely used in multiple fields during the past decades, such as politics (White at al., 2018), economic (Barnett, 2020), ecosystem (Xu et al., 2023), infectious disease (Shifa et al., 2022), and disasters (Colombi et al., 2008; Godfrey et al., 2015), etc., more and more scholars in the field of disaster studies began to pay attention to the technology of vulnerability functions, which could be rapidly assessed the risk. The vulnerability function, also known as the vulnerability curve, is a quantitative assessment method depicting the relationship between the intensity of hazard factors and the loss degree of the disaster-bearing bodies. The vulnerability function (curve) is usually represented in a two-dimensional coordinate system, where the horizontal axis represents the hazard intensity, such as rainfall intensity or wind speed, etc., and the vertical axis represents the loss degree of the disaster-bearing bodies, such as the loss rate of crops, buildings, or economic, etc. (Zhang et al., 2016).

The Application of Vulnerability Curves/Functions in the Field of Disasters

The vulnerability curve has been widely applied across various fields in recent years. It has become a crucial component in disaster assessment, quantitative risk analysis, and the creation of risk maps. Zhou et al. summarized the research progress of vulnerability curves for various disasters, including floods, earthquakes, landslides, droughts, typhoons (hurricanes) (Zhou et al., 2012). Monteleone et al. reviewed 52 articles on vulnerability curves of different crops under extreme weather events and climate change, outlining the vulnerability curve forms of different crops under conditions such as droughts, floods, and cold weather (Monteleone et al., 2023). Papathoma-Köhle et al. summarized the three analysis methods and advantages and disadvantages of physical vulnerability analysis for buildings based on debris flow disaster, including vulnerability matrices, curves, and indicators (Papathoma-Köhle et al., 2017). Vamvatsikos et al. reviewed existing concepts and methods for assessing structural vulnerability to natural disasters (earthquakes, landslides, tsunamis, and wind disasters) from a structural and engineering perspective (Vamvatsikos et al., 2010). This indicates that the application scope of vulnerability curves in the disaster domain is wide, with diverse forms and a rich variety of vulnerability assessment targets covered.

The Current Status of Vulnerability Curves in TC Risk Assessment and Loss Analysis

Nowadays, TC vulnerability function/curve method has been a widely recognized and effective method in TC risk assessment and loss analysis. There are usually two methods to establish the typhoon vulnerability function/curve - one is the engineering experiment (simulation) method, and the other is the field investigation (data inversion) method. As to the engineering experiment (simulation) method, the techniques like wind tunnel test and computer simulation are usually used to detect under what TC intensity a whole building or structural parts will fail; then, based on the original value or the reconstruction cost of the structure, the loss rate of the structure can be calculated (Zhong et al., 2017). For example, the Hazus model and the Florida hurricane model applied by the U.S. government used the structural engineering simulation to build the building vulnerability (Pinelli et al., 2011; Vickery et al., 2006a, 2006b). Compared with the engineering experiment (simulation) method, the field investigation (data inversion) method, which is based on real historical data record, is usually able to obtain data closer to the real result. Acosta et al. assessed typhoon damage in Philippine schools using empirical vulnerability curves, based on damage quantification against maximum local wind speeds (Acosta et al., 2018). Zhu et al. developed a road vulnerability model against TCs in Hainan Province, using historical road damage data and historical TC intensity measures like precipitation and wind speed (Zhu et al., 2022).

Despite numerous studies on TC vulnerability functions, it should be noted that TC vulnerability functions often differ across regions due to the geographical spatiotemporal heterogeneity. Limited by the availability of research data, many studies only focus on a specific province or city without comparing differences between different regions. In some practical applications, there have been cases where the typhoon vulnerability curve of a certain province has been used to assess losses in another province when the historical data records of the latter is inaccessible, introducing significant human error into typhoon damage assessments. Therefore, developing a library of typhoon vulnerability functions suitable for different regions has become a worthwhile hotspot in this field.

THE OVERALL STRUCTURE

The overall structure of this study is shown in Figure 1. The region studied comprises twelve coastal provinces and provinces adjacent to coastal provinces in China, having a characteristic of being vulnerable to typhoons. The basic data by province and a 15-year-long typhoon dataset in all provinces, including disaster intensity and losses caused by TCs, are collected. Based on the basic dataset, six alternative vulnerability functions are calibrated to fit the loss rates of the economic, population, and farmland in each province, respectively, and finally, the optimal vulnerability functions are selected to profile the losses caused by typhoons. The heterogeneity of the losses of different disaster-bearing bodies in different provinces along the coastal areas in China are analyzed. The results provided by this paper could provide a profound understanding of typhoon disasters in coastal areas in China, and also the reference and technological support for the government emergency management to cope with typhoon disasters.

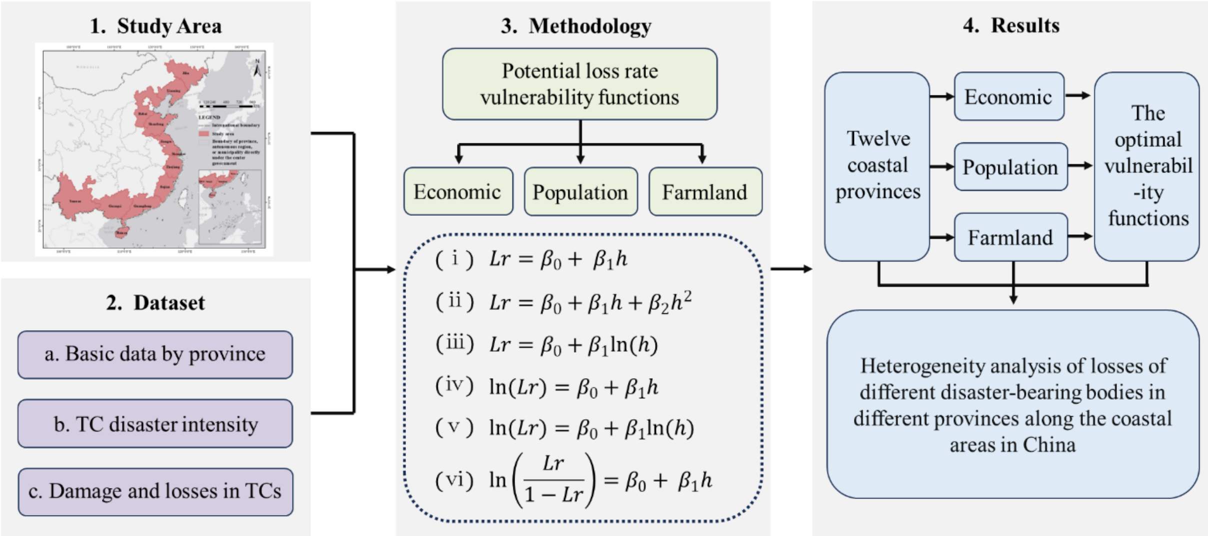

Figure 1. The Overall Structure of This Study

STUDY AREA AND DATASETS

Study Area

"China Marine Statistical Yearbook" defines coastal areas as regions with coastlines, including both categories of mainland coastlines and island coastlines (Ministry of Natural Resources of the People's Republic of China, 2017). According to this definition, ten coastal provinces in China are considered in this paper, including Liaoning, Hebei, Shandong, Jiangsu, Shanghai, Zhejiang, Fujian, Guangdong, Guangxi, and Hainan. According to the historical records of typhoon-related disasters and the impact of typhoons, Jilin Province and Yunnan Province are also tagged as provinces prone to typhoons, so these two provinces are also included in the scope of this study. Due to the data availability issue, Tianjin Province, Taiwan Province, Hong Kong Special Administrative Region (SAR) and Macao SAR are temporarily not taken into account in this paper. Summarily, this study includes 12 provinces in total. Figure 2 illustrates the study area in this study.

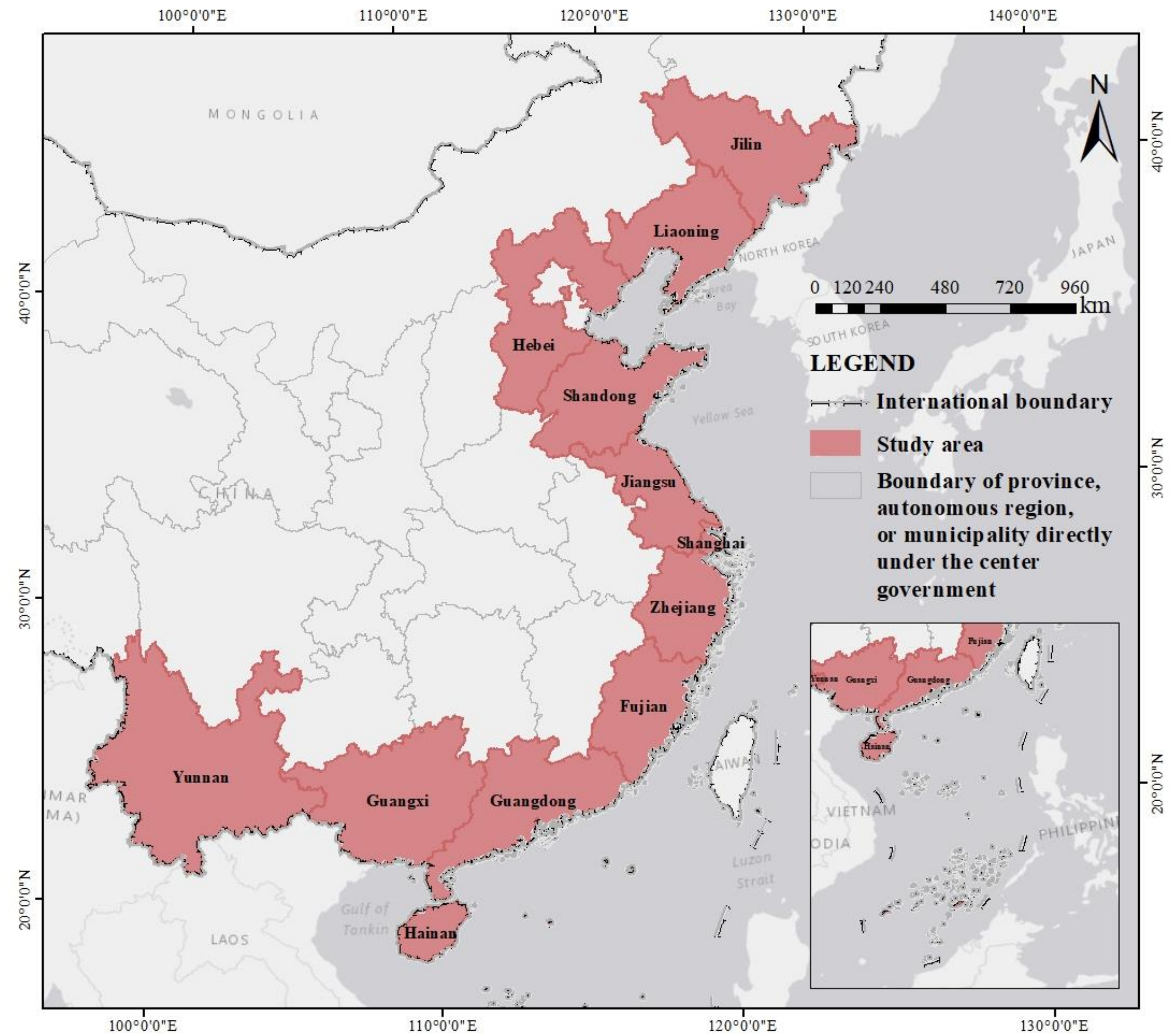

Figure 2. The Study Area in This Study

The basic situations of all the provinces involved in this study are shown in Table 1. It should be noted that the number of meteorological stations in Table 1 refers to the number of the stations which have ever reported the total cumulative rainfall during the typhoons. Stations that do not give records are not counted. The precipitation data from multiple meteorological stations consider the spatial heterogeneity of total rainfall in each province. A total of 451 typhoons with recorded disasters occurred in 22 provinces in China from 2003 to 2018. Among them, the 12 provinces selected for this study experienced a total of 357 typhoon events, indicating that this region is under serious threat of typhoon disasters.

Table 1. Basic Overview of The Study Area (Using Data in 2018)

Province	Gross Regional Product (100 million yuan)	Population (10000 persons)	Total Sown Area (1000 hectares)	Number of meteorological stations	Number of typhoons from 2003 to 2018
Jilin	15074.6	2704	6080.9	6	5
Liaoning	25315.4	4359	4207.1	5	12
Hebei	36010.3	7556	8197.1	5	9
Shandong	76469.7	10047	11076.8	6	16
Jiangsu	92595.4	8051	7520.2	7	21
Shanghai	32679.9	2424	282.3	1	17
Zhejiang	56197.2	5737	1978.7	5	44
Fujian	35804	3941	1577.3	3	59

Guangdong	97277.8	11346	4279.4	7	69
Guangxi	20352.5	4926	5972.4	6	45
Hainan	4832.05	934	712.9	2	45
Yunnan	17881.1	4830	6890.8	8	15

Datasets

Since the precipitation data for each typhoon is only available until 2018, this study covers a period of 15 years from 2003 to 2018. The basic data by province, such as gross regional product (GRP), population, and sown area are obtained from the “China Statistical Yearbook” (National Bureau of Statistics of China, 2004-2019). The total precipitation caused by individual typhoons, a factor contributing to disasters, is extracted from the Tropical Cyclone Data Center of the China Meteorological Administration (Ying et al., 2014; Lu et al., 2021). The typhoon disaster loss data, including direct economic losses, affected population, and affected crop area, are sourced from the “Yearbook of Meteorological Disasters in China” (China Meteorological Administration, 2004-2019). All the involved data is publicly available, and the authors have placed download links of all the data in References section.

METHODOLOGY

The alternative forms of the TC vulnerability functions considered in this paper are inspired by the work by Jiang et al. (Jiang et al., 2023). The general form of the vulnerability regression model with the loss rate as the dependent variable is as follows:

$$g(Lr) = f(h) + \varepsilon, \varepsilon \sim N(0, \sigma^2) \quad (1)$$

Where Lr denotes the loss rate; $g(Lr)$ denotes the transformation function of the dependent variable Lr; h denotes the hazard intensity that serves as the independent variable; $f(h)$ denotes the regression function of the independent variable h. The function $f(h)$ may depend on several parameters, denoted by β_0, β_1, etc., which remain to be estimated. ε denotes the random error term, usually conforming to the normal distribution.

Vulnerability regression models can be categorized into three main types: linear models, logarithmic models and probability curve model.

Linear Models

The linear model does not transform the dependent variable (the loss rate) to other mathematical forms. That is, $g(Lr) = Lr$. The linear models comprise three forms, namely simple linear model, polynomial model, linear-logarithmic model. The formulas are as follows, respectively.

$$Lr = \beta_0 + \beta_1 h \quad (2)$$

$$Lr = \beta_0 + \beta_1 h + \beta_2 h^2 \quad (3)$$

$$Lr = \beta_0 + \beta_1 \ln(h) \quad (4)$$

where: β_1 denotes the slope parameter, indicating the degree and trend of the change in the loss rate with change in hazard intensity. β_0 denotes the intercept parameter, representing the baseline loss rate when the hazard indicator is zero. In formula (3) β_2 denotes quadratic term. It should be noted that, although a non-zero intercept term is challenging to interpret, β_0 is not forced to be zero in this study. The main reason for this is that the cumulative rainfall intensity during a typhoon, which is selected as an indicator for hazard intensity, may not paint the full picture of that typhoon. Therefore, setting the parameter β_0 artificially to zero may not make sense.

Logarithmic Models

Logarithmic models involve the operation of taking the logarithm of the dependent variable Lr, that is, $g(Lr) = \ln(Lr)$. The logarithmic models comprise two forms, namely logarithmic-linear model and logarithmic-logarithmic model. The formulas are as follows, respectively.

$$\ln(Lr) = \beta_0 + \beta_1 h \quad (5)$$

$$\ln(Lr) = \beta_0 + \beta_1 \ln(h) \quad (6)$$

where: the slope parameter β_1 in Formula (5) and Formula (6) represents the absolute change and the relative change in hazard intensity, respectively.

Probability Curve Model

Linear models and logarithmic models cannot guarantee that the predicted values of the loss rate will fall entirely within the interval of [0, 1]. In order to overcome this shortcoming, another function form is introduced here which takes the logarithm of the ratio of the loss rate Lr to $(1 - Lr)$. This model is named as logistic curve model. The formula is as follows.

$$\ln\left(\frac{Lr}{1 - Lr}\right) = \beta_0 + \beta_1 h \tag{7}$$

RESULTS

The Optimal Vulnerability Functions of Economic, Population, and Crop in Different Provinces

The refined data of all single typhoons transiting the study area from 2003 to 2018 were collected in this study. The accumulated rainfall during the typhoons at various meteorological stations were compiled as the independent variable. For all the 12 provinces, three kinds of disaster-bearing bodies are considered, including economic, population, and crops. The data of the disaster-bearing bodies were normalized by dividing the loss values by the total amount, that is, the area of affected crop is divided by the sown area; the affected population is divided by the year-end population; and the economic loss is divided by the year-end GDP, respectively. Finally, the economic loss rate, the affected population rate, and the affected crop rate were obtained and then considered as the dependent variables in this study.

The provincial data were fitted to alternative vulnerability models introduced in Methodology section and the optimal vulnerability function was finally selected by comparing the R-squared values of different curves. A 95% confidence interval was plotted for each optimal vulnerability curve to depict the potential range of $f(h)$ at a 95% confidence level. The aggregated results of all the optimal vulnerability functions are presented in Table 2 below.

Table 2. The Vulnerability Functions of Economic, Population, and Crop in Different Provinces

Prov.	Economic Loss Rate	Affected Population Rate	Affected Crop Rate
Jilin	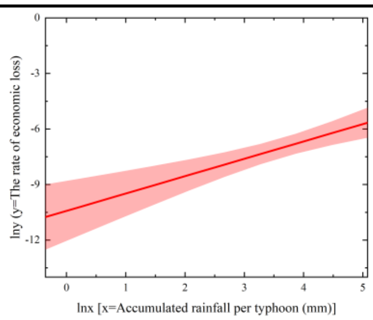 $\ln(Lr) = \beta_0 + \beta_1 \ln(h)$, β_0 = -10.42$\pm$0.77; β_1 = 0.94$\pm$0.20	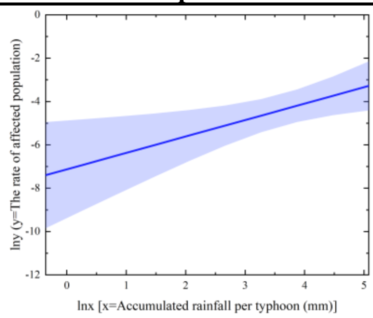 $\ln(Lr) = \beta_0 + \beta_1 \ln(h)$, β_0 = -7.13$\pm$1.08; β_1 = 0.76$\pm$0.28	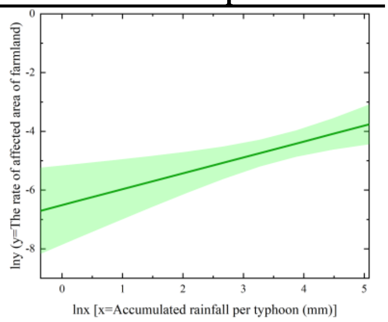 $\ln(Lr) = \beta_0 + \beta_1 \ln(h)$, β_0 = -6.51$\pm$0.64; β_1 = 0.54$\pm$0.17
Liaoning	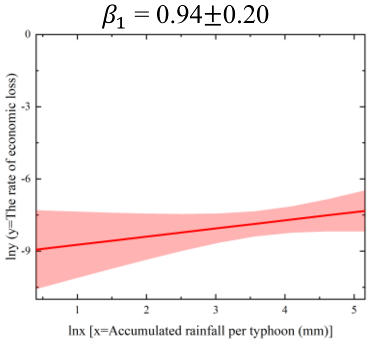 $\ln(Lr) = \beta_0 + \beta_1 \ln(h)$, β_0 = -9.08$\pm$0.90; β_1 = 0.34$\pm$0.23	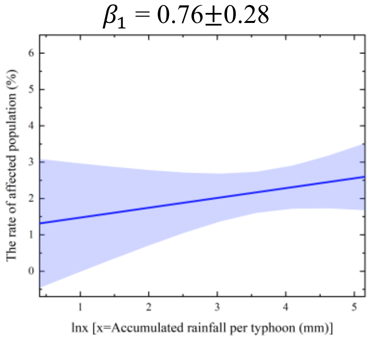 $Lr = \beta_0 + \beta_1 \ln(h)$, β_0 = 1.21E-2$\pm$9.74E-3; β_1 = 2.70E-3$\pm$2.51E-3	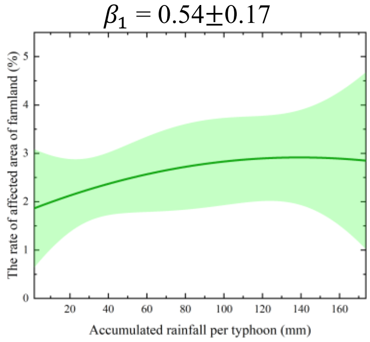 $Lr = \beta_0 + \beta_1 h + \beta_2 h^2$, β_0 = 1.84E-2$\pm$6.30E-3; β_1 = 1.55E-4$\pm$2.00E-4; β_2 = -5.56E-7$\pm$1.17E-6

Prov.	Economic Loss Rate	Affected Population Rate	Affected Crop Rate
Hebei	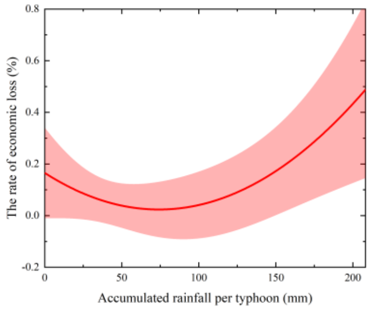 $Lr = \beta_0 + \beta_1 h + \beta_2 h^2$, β_0 = 1.66E-3±8.37E-4; β_1 = -3.83E-5±2.20E-5; β_2 = 2.58E-7±1.09E-7	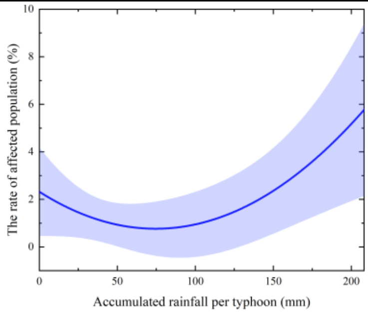 $Lr = \beta_0 + \beta_1 h + \beta_2 h^2$, β_0 = 2.32E-2±8.86E-3; β_1 = -4.18E-4±2.32E-4; β_2 = 2.80E-6±1.16E-6	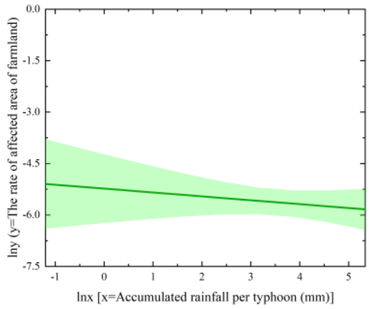 $\ln(Lr) = \beta_0 + \beta_1 \ln(h)$, β_0 = -5.23±0.48; β_1 = -0.11±0.13
Shandong	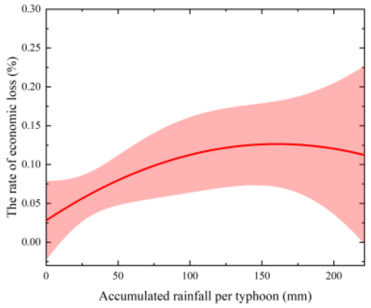 $Lr = \beta_0 + \beta_1 h + \beta_2 h^2$, β_0 =2.80E-4±2.56E-4; β_1 = 1.23E-5±7.73E-6; β_2 = -3.82E-8±3.80E-8	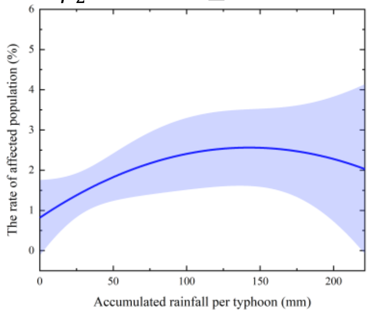 $Lr = \beta_0 + \beta_1 h + \beta_2 h^2$, β_0 = 8.19E-3±4.70E-3; β_1 = 2.45E-4±1.42E-4; β_2 = -8.58E-7±6.97E-7	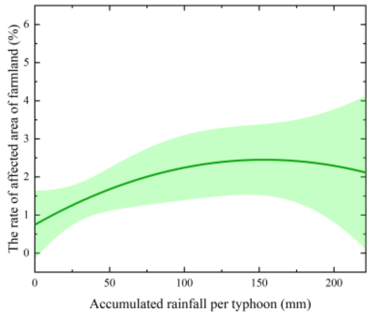 $Lr = \beta_0 + \beta_1 h + \beta_2 h^2$, β_0 = 7.43E-3±4.49E-3; β_1 = 2.23E-4±1.36E-4; β_2 = -7.27E-7±6.66E-7
Jiangsu	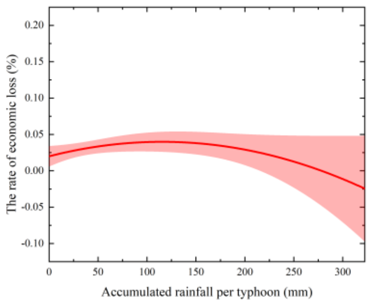 $Lr = \beta_0 + \beta_1 h + \beta_2 h^2$, β_0 = 1.99E-4±7.13E-5; β_1 = 3.46E-6±1.70E-6; β_2 = -1.50E-8±7.52E-9	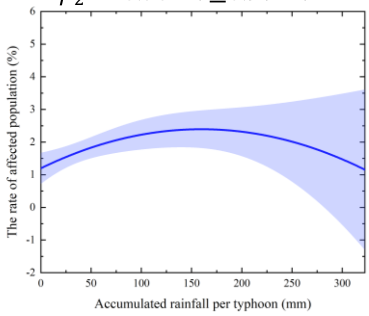 $Lr = \beta_0 + \beta_1 h + \beta_2 h^2$, β_0 = 1.20E-2±2.40E-3; β_1 = 1.50E-4±5.81E-5; β_2 = -4.69E-7±2.53E-7	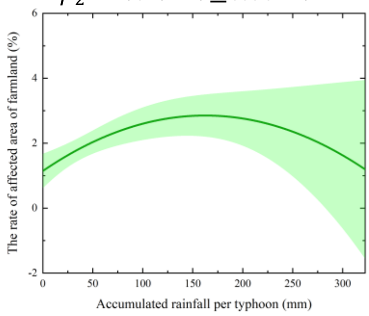 $Lr = \beta_0 + \beta_1 h + \beta_2 h^2$, β_0 = 1.14E-2±2.67E-3; β_1 = 2.10E-4±6.46E-5; β_2 = -6.48E-7±2.82E-7
Shanghai	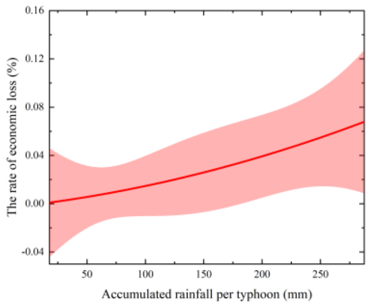 $Lr = \beta_0 + \beta_1 h + \beta_2 h^2$, β_0 = -1.29E-5±2.78E-4; β_1 = 1.17E-6±4.68E-6; β_2 = 4.31E-9±1.49E-8	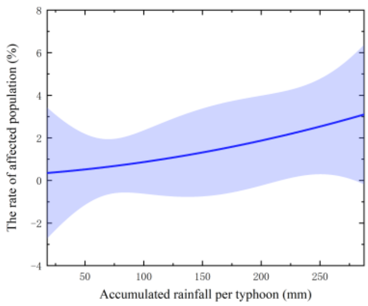 $Lr = \beta_0 + \beta_1 h + \beta_2 h^2$, β_0 = 2.78E-3±1.86E-2; β_1 = 3.78E-5±3.07E-4; β_2 = 2.10E-7±9.47E-7	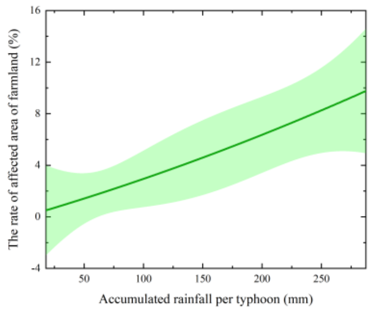 $Lr = \beta_0 + \beta_1 h + \beta_2 h^2$, β_0 = 1.90E-4±2.19E-2; β_1 = 2.68E-4±3.92E-4; β_2 = 2.47E-7±1.26E-6

Prov.	Economic Loss Rate	Affected Population Rate	Affected Crop Rate
Zhejiang	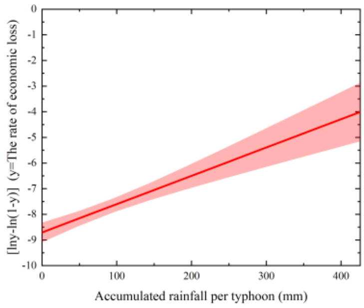	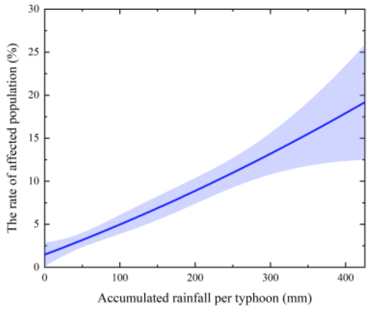	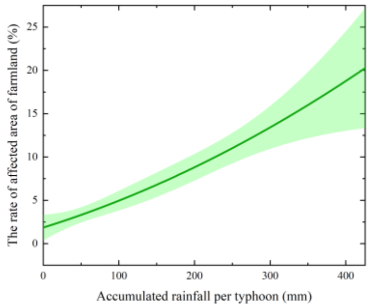
	$\ln\left(\frac{Lr}{1-Lr}\right) = \beta_0 + \beta_1 h,$ β_0 = -8.71±0.19; β_1 = 1.10E-2±1.64E-3	$Lr = \beta_0 + \beta_1 h + \beta_2 h^2,$ β_0 = 1.47E-2±7.04E-3; β_1 = 3.30E-4±1.36E-4; β_2 = 2.03E-7±4.41E-7	$Lr = \beta_0 + \beta_1 h + \beta_2 h^2,$ β_0 = 1.85E-2±7.55E-3; β_1 = 2.73E-4±1.43E-4; β_2 = 3.75E-7±4.59E-7
Fujian	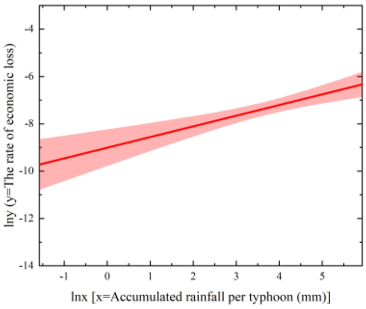	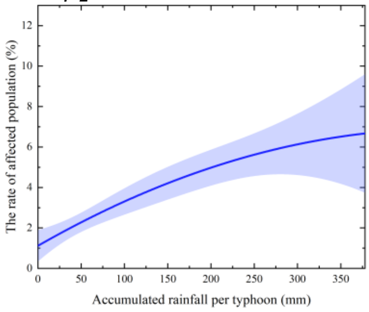	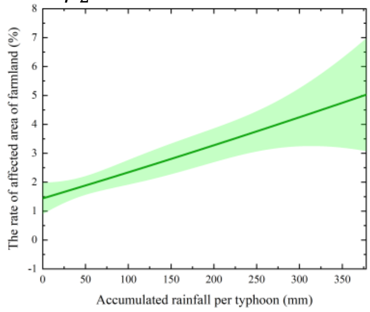
	$\ln(Lr) = \beta_0 + \beta_1 \ln(h),$ β_0 = -9.01±0.39; β_1 = 0.45±0.10	$Lr = \beta_0 + \beta_1 h + \beta_2 h^2,$ β_0 = 1.12E-2±3.91E-3; β_1 = 2.45E-4±7.90E-5; β_2 = -2.59E-7±2.63E-7	$Lr = \beta_0 + \beta_1 h + \beta_2 h^2,$ β_0 = 1.44E-2±2.77E-3; β_1 = 8.85E-5±5.36E-5; β_2 = 1.69E-8±1.77E-7
Guangdong	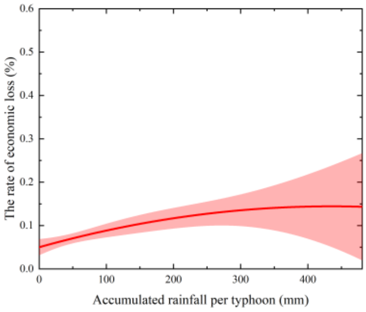	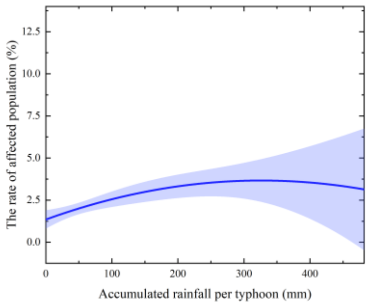	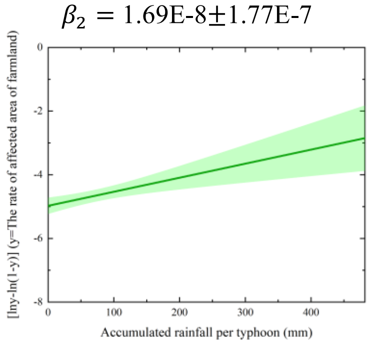
	$Lr = \beta_0 + \beta_1 h + \beta_2 h^2,$ β_0 = 5.01E-4±9.50E-5; β_1 = 4.33E-6±1.82E-6; β_2 = -4.98E-9±5.61E-9	$Lr = \beta_0 + \beta_1 h + \beta_2 h^2,$ β_0 = 1.35E-2±2.78E-3; β_1 = 1.42E-4±5.32E-5; β_2 = -2.18E-7±1.63E-7	$\ln\left(\frac{Lr}{1-Lr}\right) = \beta_0 + \beta_1 h,$ β_0 = -4.97±0.13; β_1 = 4.41E-3±1.25E-3
Guangxi	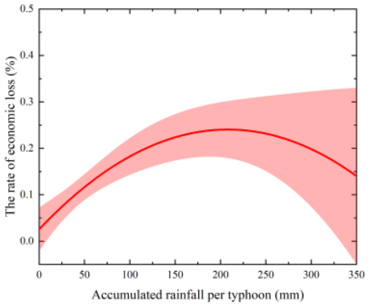	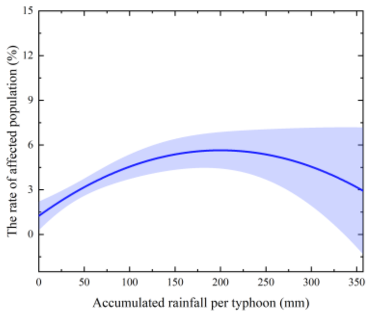	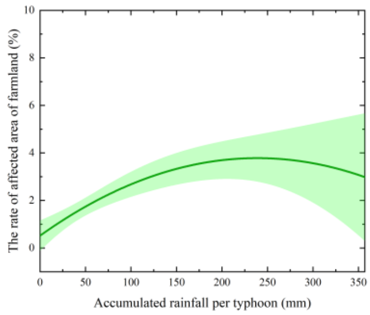
	$Lr = \beta_0 + \beta_1 h + \beta_2 h^2,$ β_0 = 2.54E-4±2.39E-4; β_1 = 2.07E-5±5.10E-6; β_2 = -4.97E-8±1.85E-8	$Lr = \beta_0 + \beta_1 h + \beta_2 h^2,$ β_0 = 1.24E-2±4.87E-3; β_1 = 4.41E-4±1.06E-4; β_2 = -1.10E-6±3.89E-7	$Lr = \beta_0 + \beta_1 h + \beta_2 h^2,$ β_0 =5.17E-3±3.25E-3; β_1 = 2.73E-4±6.87E-5; β_2 = -5.73E-7±2.48E-7

Prov.	Economic Loss Rate	Affected Population Rate	Affected Crop Rate
Hainan	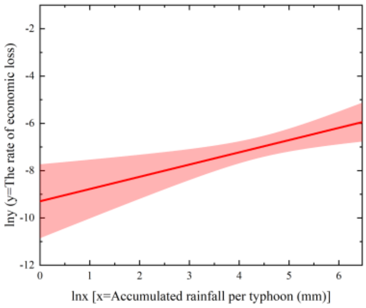 $\ln(Lr) = \beta_0 + \beta_1 \ln(h)$, β_0 = -9.29$\pm$0.79; β_1 = 0.52$\pm$0.17	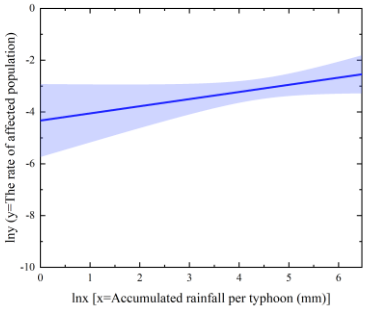 $\ln(Lr) = \beta_0 + \beta_1 \ln(h)$, β_0 = -4.33$\pm$0.71; β_1 = 0.28$\pm$0.15	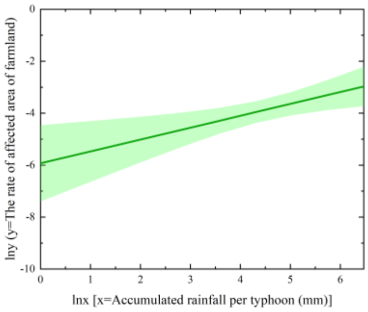 $\ln(Lr) = \beta_0 + \beta_1 \ln(h)$, β_0 = -5.93$\pm$0.74; β_1 = 0.46$\pm$0.16
Yunnan	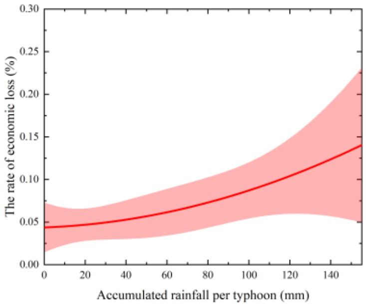 $Lr = \beta_0 + \beta_1 h + \beta_2 h^2$, β_0 = 4.37E-4$\pm$1.47E-4; β_1 = 9.17E-7$\pm$6.42E-6; β_2 = 3.43E-8$\pm$5.02E-8	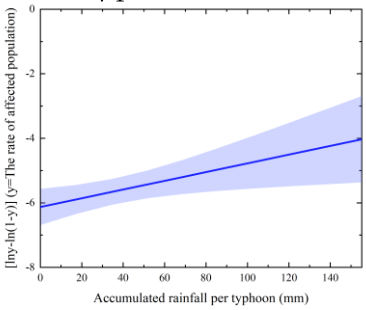 $\ln\left(\frac{Lr}{1-Lr}\right) = \beta_0 + \beta_1 h$, β_0 = -6.13$\pm$0.28; β_1 = 1.35E-2$\pm$5.42E-3	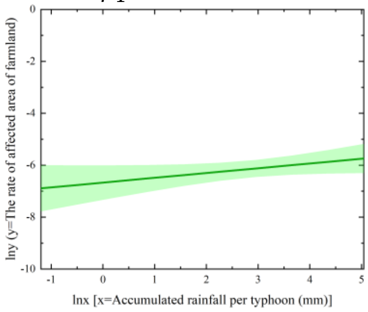 $\ln(Lr) = \beta_0 + \beta_1 \ln(h)$, β_0 = -6.67$\pm$0.33; β_1 = 0.18$\pm$0.10

It can be seen from Table 2 that the optimal vulnerability functions for all the three disaster-bearing bodies mainly concentrate on two categories: polynomial model and logarithmic-logarithmic model, accounting for 64% and 25% of the total, respectively. It means that the polynomial model and logarithmic-logarithmic model can more effectively capture the nonlinear relationship between the disaster intensity and the loss rate of the disaster-bearing bodies, thereby showing better fitting performance.

It is found that the optimal vulnerability function forms for the three disaster-bearing bodies may vary even in the same province. For instance, the vulnerability function types for the three disaster-bearing bodies are the same in Jilin, Shandong, Jiangsu, Shanghai, Guangxi, and Hainan, while differ from one another in all the other provinces. Therefore, when studying vulnerability of different disaster-bearing bodies in a specific region, the optimal vulnerability function type should be chosen based on the actual fitting performance, and it is not advisable to simply use a single type of vulnerability function for analysis.

For the provinces of Jilin, Shandong, Jiangsu, Shanghai, Guangxi, and Hainan, despite that all the three vulnerability functions have the consistent form, the parameters from the curve fitting are not the same, indicating that the loss rate variabilities of different disaster-bearing bodies are not the same. Taking Hainan Province as an example, the vulnerability function forms of economic, population, and crop conform to logarithmic-logarithmic model while the parameter β_1 in the models are different, showing the following rules: β_1 of the economic loss rate model > β_1 of the affected crop rate model > β_1 of the affected population rate model. The results suggest that changes in the typhoon intensity have different impact mode and degree on different disaster-bearing bodies.

Comparative analysis of the vulnerability functions of the same disaster-bearing body in different provinces reveals that the styles of vulnerability functions usually vary for different regions, even when the optimal fitting vulnerability function types are consistent. For example, Jilin, Liaoning, Fujian, and Hainan share the same form of vulnerability function while the key parameters in the functions are diverse from each other, with β_1 in the model in Jilin > β_1 in the model in Hainan > β_1 in the model in Fujian > β_1 in the model in Liaoning. This reflects that the resilience of different provinces to typhoon disasters could be different.

The Vulnerability Heterogeneity of Economic, Population, and Crop in Different Provinces

Preliminary conclusions can be drawn by comparing the size of key parameters when the same vulnerability function form is applied in different disaster-bearing bodies in different provinces, but it is difficult to carry out comparative studies intuitively for different vulnerability function forms. To solve this problem, further visual analysis of the loss rates and predicted loss values (based on the 2018 data) of the three disaster-bearing bodies in 12 provinces under the same disaster intensity is conducted (Figure 3), so as to see the vulnerability heterogeneity of economic, population, and crop in different provinces more directly. It can be seen from Figure 3 that the loss rates and predicted loss values of all the three disaster-bearing bodies generally increase with the increase of the accumulated rainfall during the typhoon, suggesting that more severe disasters can bring greater losses, which is consistent with people's perception. More specifically, there are the following important findings.

As to the heterogeneity of economic loss rate in extreme typhoon-rainfall scenarios in different provinces, it can be seen from Figure 3(a) that Hebei, Jilin, Zhejiang, and Yunnan top the list. It can be seen from Table 1 above that among these provinces, Hebei, Jilin, and Yunnan have the fewest typhoons per year on average. It can be reasonable to speculate that these provinces may be less prepared for typhoons since typhoons are not frequent in history, resulting in greater impacts when typhoons occur. It reminds us that relevant departments should deal with extreme disasters such as typhoons that occur infrequently. Figure 3(b) shows that Hebei, Zhejiang, Guangdong, Jilin, and Yunnan top the list of the predicted total economic loss in extreme typhoon-rainfall scenarios. The ranking of the predicted total economic loss does not change much in general, while of course the ranking of provinces with large Gross Regional Product, such as Guangdong, will rise.

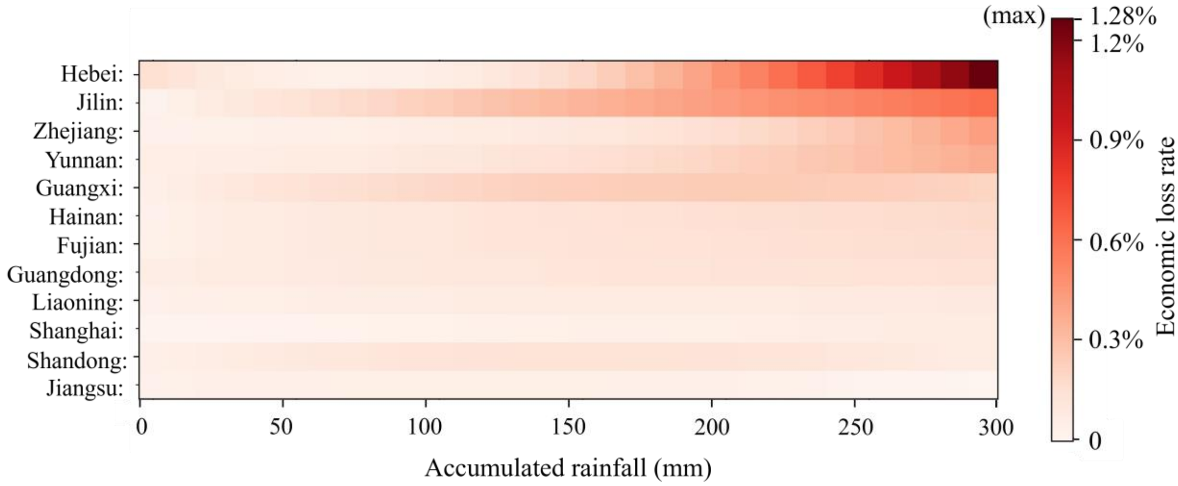

(a) Economic loss rate under the same scenario of typhoon-induced rainfall

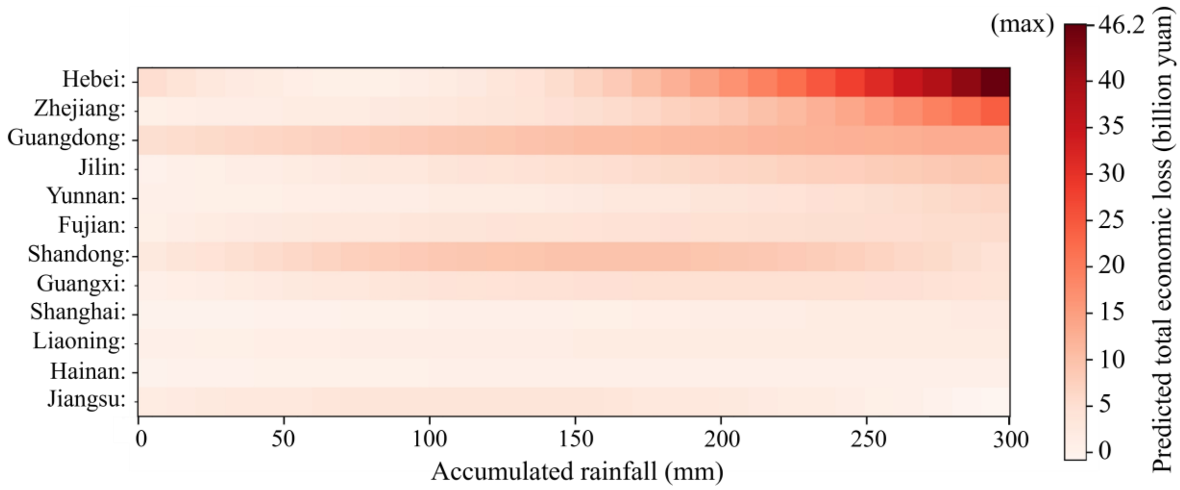

(b) Predicted total economic loss under the same scenario of typhoon-induced rainfall

Figure 3. Heterogeneity of Economic Loss in Different Provinces

As to the heterogeneity of affected population rate in extreme typhoon-rainfall scenarios in different provinces, it can be seen from Figure 4(a) that Hebei, Zhejiang, Yunnan, Hainan, and Jilin top the list. This finding is highly consistent with the finding related to economic loss, suggesting a high similarity degree between the vulnerability of the affected population and the vulnerability of the economic system in these provinces, most of which have experienced less typhoon damage in the history. It can be seen from Figure 4(b) that Hebei, Zhejiang, Yunnan, Guangdong, Fujian top the list of predicted total affected population in extreme typhoon-rainfall scenarios in different provinces. Considering that Guangdong has 113.46 million population and Fujian has 39.41 million population, which are significantly larger than the population in Hainan (9.34 million population) and Jilin (27.04 million population), this result is not difficult to understand.

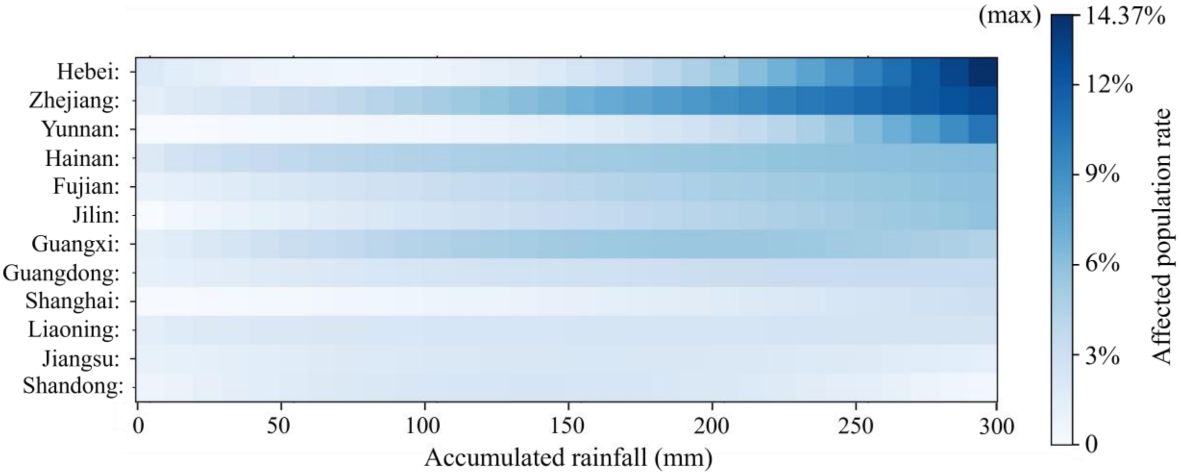

(a) Affected population rate under the same scenario of typhoon-induced rainfall

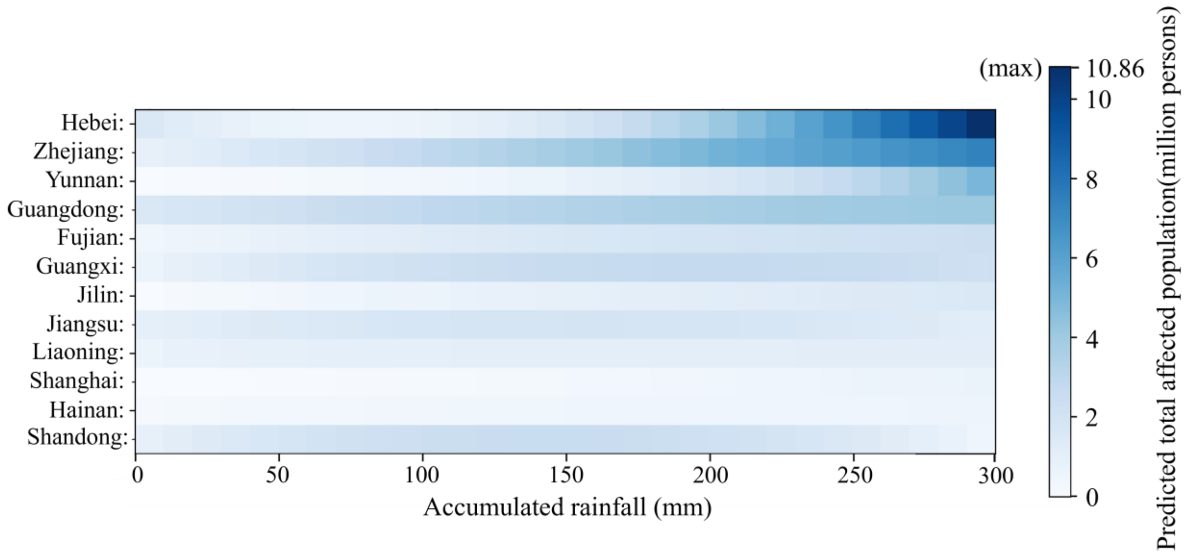

(b) Predicted total affected population under the same scenario of typhoon-induced rainfall

Figure 4. Heterogeneity of Affected Population in Different Provinces

As to the heterogeneity of affected crop rate in extreme typhoon-rainfall scenarios in different provinces, it can be seen from Figure 5(a) that Zhejiang and Shanghai top the list, with obviously larger value of affected crop rate. However, the pattern in Figure 5(b) is a little more complex. Firstly, the predicted total affected crop area in Shanghai is very small, only ranking the fourth from bottom. The main reason for this phenomenon is that Shanghai, as a modern metropolis, has almost no agricultural production. The total sown area in Shanghai is only 282.3×10^3 hectares, and the sown area is even less than 1/10 of that of some provinces. Despite that the affected crop rate in extreme typhoon-rainfall scenarios in Shanghai is huge, the overall crop loss is small. Secondly, due to the regional differences in the crop area, many provinces, although the crop loss rate is small, the total crop loss under extreme typhoon-rainfall scenarios could be large. These provinces include Guangxi (4th in loss rate; 2nd in loss), Jilin (6th in loss rate; 3rd in loss), Jiangsu (8th in loss rate; 4th in loss), and Shandong (10th in loss rate; 5th in loss). These provinces have a common feature that they are traditionally large agricultural provinces, with a large area of cultivation. Therefore, only the affected crop rate cannot accurately reflect the overall situation of agricultural damage while total affected crop area could be a more accurate indicator. Thirdly, it is found that Zhejiang Province is a typical province with severe agricultural damage under typhoon disasters. Not only the crop loss rate is high in Zhejiang, but also the total crop loss value is extremely large.

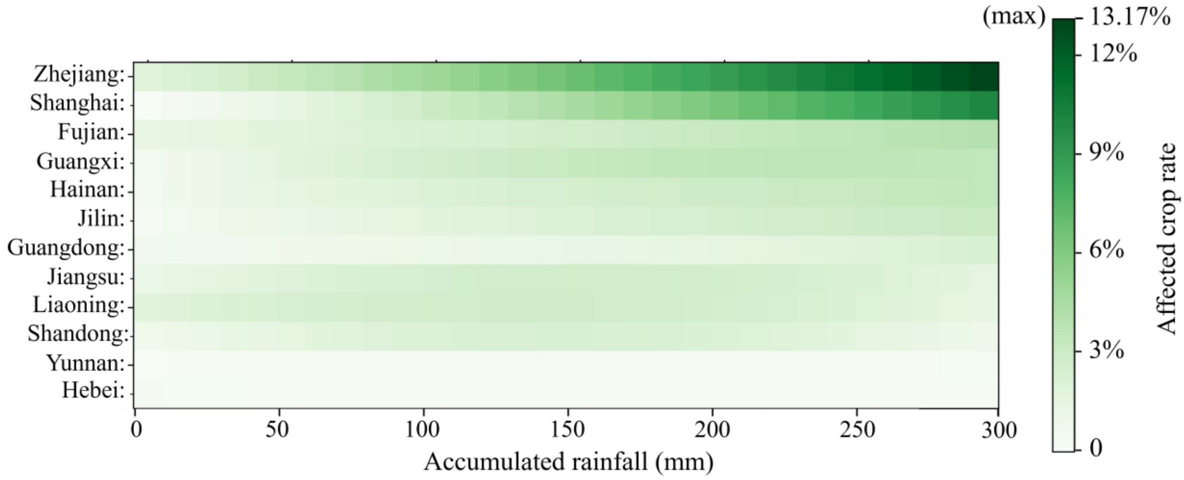

(a) Affected crop rate under the same scenario of typhoon-induced rainfall

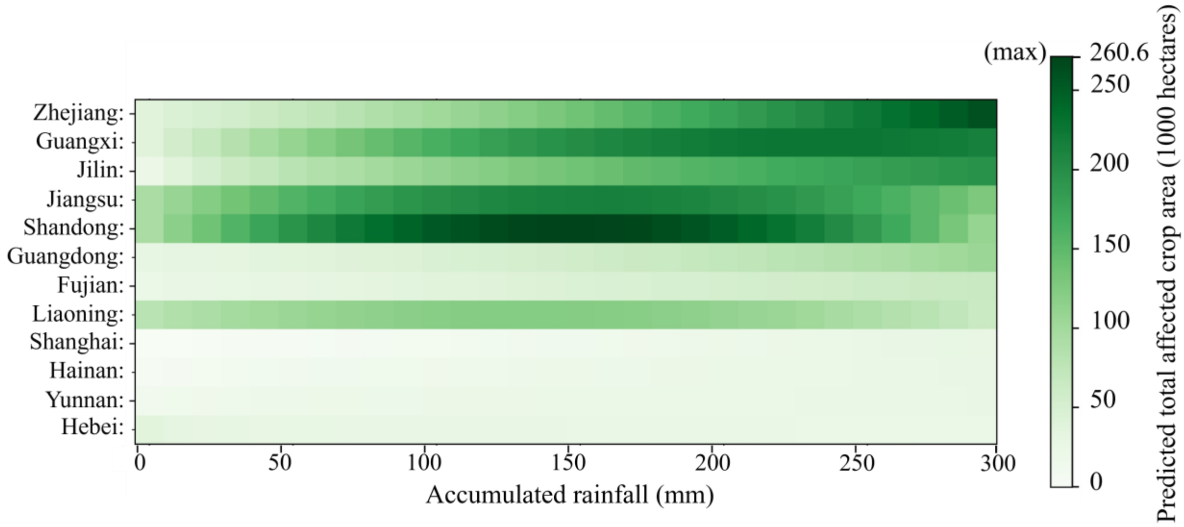

(b) Predicted total affected crop area under the same scenario of typhoon-induced rainfall

Figure 5. Heterogeneity of Affected Crop Area in Different Provinces

LIMITATIONS AND FUTURE WORK

Limitation in The Selection of Disaster Indicator

When a typhoon passes through, there are often multiple dimensions of disaster indicators. As a preliminary study, only cumulative rainfall during the typhoon transit was selected as the indicator of disaster intensity due to the accessibility of the data in this study, and other indicators were not considered temporarily. In the further study, we plan to furtherly investigate the applicability of other disaster indicators as the independent variable in TC vulnerability function construction for a more accurate and comprehensive typhoon risk assessment.

Limitation in The Selection of Potential TC Vulnerability Functions

Appropriate choice of the potential vulnerability curve forms is the basis for developing effective vulnerability curves. In this study, the six potential vulnerability functions suggested by the work by Jiang et al. (2023) were mainly referred to. The authors plan to test more forms of vulnerability functions, and hope that more regionally applicable vulnerability curves might be found in near future.

Limitation in Limited Number of Data Samples in Domain of High Disaster Intensity

Higher disaster intensity typically results in greater losses. However, fewer data points from infrequent high-intensity typhoons can disrupt curve accuracy, which causes the problem that the vulnerability curve does not increase monotonously. The authors plan to accumulate typhoon data over a longer period of time, thereby increasing the number of high-intensity-value points to obtain more accurate fitting results.

CONCLUSIONS

Tropical cyclones are one of the natural disasters with high frequency, strong destructive power, and widespread global impact. The southeast coastal area of China is the most economically developed and densely populated area in China, and is also a typhoon-prone area. Therefore, conducting a disaster-bearing body vulnerability assessment in the coastal areas of China is imperative. Based on the collected disaster data in 12 provincial-level coastal regions in China from 2003 to 2018, this study selected accumulated rainfall during the typhoons as the causative factor. The direct economic loss rate, affected population rate, and affected crop rate were selected as the indexes of the disaster outcome. Through the construction, fitting, and comparation of six alternative regression-based vulnerability functions, the optimal vulnerability functions for three disaster-bearing bodies in 12 provinces in were identified.

It was found in this study that the optimal vulnerability curves for all the disaster-bearing bodies are mainly concentrated in polynomial model and logarithmic-logarithmic model, accounting for 64% and 25% of the total, respectively, which shows that these two models could be the most suitable choice for the application of vulnerability assessment in the study area. It was also found that the constructed vulnerability curves generally exhibit a monotonically increasing trend, indicating that losses continuously increase with the increase of cumulative typhoon rainfall. As to the heterogeneity in different provinces, it was found that Hebei, Jilin, Zhejiang, Yunnan, and Hainan top the list of economic loss rate and affected population rate, while most of them have the fewest typhoons per year on average. It indicates that the economic loss and the population suffering condition may be severer in the provinces where typhoons are not common relatively, probably since these provinces were less well prepared for typhoons. Also, it was found that the provincial differences in crop loss rates and crop loss values are very large. The loss rate in large agricultural provinces is not high, but the absolute loss value could be very large, reflecting that crop losses are very dependent on the size of agricultural acreage, rather than solely determined by the loss rates.

As a preliminary study, there are still some limitations in this paper. To the best of the authors' knowledge, this paper gives a first attempt in exploring the optimal vulnerability functions for coastal provinces in China. The relevant results from this paper are of great significance for understanding the spatial heterogeneity of typhoon disasters and disaster victims. This paper could also provide valuable references for government departments in implementing accurate typhoon risk assessment, and improving disaster prevention and response capabilities.

ACKNOWLEDGMENTS

This work was supported by National Natural Science Foundation of China (Grant No. 72304038), Guangdong Basic and Applied Basic Research Foundation (Grant No. 2022A1515110049), Young Innovative Talents Project from Department of Education of Guangdong Province (Grant No. 2022KQNCX157).

DATA AVAILABILITY STATEMENT

All the data used in this article are provided with references and links at the manuscript.

REFERENCES

Academy of Disaster Reduction and Emergency Management, National Disaster Reduction Centre of China, International Federation of Red Cross and Red Crescent Societies (IFRC), Beijing Normal University. (2023). 2022 Global natural disaster assessment report. https://www.preventionweb.net/publication/2022-global-natural-disaster-assessment-report

Acosta, T.J.S., Galisim, J.J., Tan, L.R., Hernandez, J.Y. (2018). Development of empirical wind vulnerability curves of school buildings damaged by the 2016 Typhoon Nina. *Procedia Engineering*, *212*, 395-402. https://doi.org/10.1016/j.proeng.2018.01.051

Barnett, J. (2020). Global environmental change II: Political economies of vulnerability to climate change. *Progress in Human Geography*, *44*(6), 1172-1184. https://doi.org/10.1177/0309132519898254

China Meteorological Administration. (2004-2019). Yearbook of Meteorological Disasters in China. https://data.cnki.net/statisticalData/index?ky=%E4%B8%AD%E5%9B%BD%E6%B0%94%E8%B1%A1%E7%81%BE%E5%AE%B3%E5%B9%B4%E9%89%B4

Colombi, M., Borzi, B., Crowley, H., Onida, M., Meroni, F., & Pinho, R. (2008). Deriving vulnerability curves using Italian earthquake damage data. *Bulletin of Earthquake Engineering*, *6*, 485-504. https://doi.org/10.1007/s10518-008-9073-6

Godfrey, A., Ciurean, R.L., van Westen, C.J., Kingma, N.C., & Glade, T. (2015). Assessing vulnerability of buildings to hydro-meteorological hazards using an expert based approach - An application in Nehoiu Valley, Romania. *International Journal of Disaster Risk Reduction*, *13*, 229-241. https://doi.org/10.1016/j.ijdrr.2015.06.001

Jiang, X.Y., Ma, X.Y., & Yang, L.J. (2023). Comprehensive comparative study on the construction method of flood vulnerability and fragility curves under the framework of regression analysis. *Shuili Xuebao*, *54*(2), 184-198. https://doi.org/10.13243/j.cnki.slxb.20220307 [in Chinese]

Lee, T.C., Knutson, T.R., Nakaegawa, T., Ying, M., & Cha, E.J. (2020). Third assessment on impacts of climate change on tropical cyclones in the Typhoon Committee Region - Part I: Observed changes, detection and attribution. *Tropical Cyclone Research and Review*, *9*(1), 1-22. https://doi.org/10.1016/j.tcrr.2020.03.001

Lu, X. Q., Yu, H., Ying, M., Zhao, B.K., Zhang, S., Lin, L.M., Bai, L.N., & Wan, R.J. (2021). Western North Pacific tropical cyclone database created by the China Meteorological Administration. *Advances in Atmospheric Sciences*, *38*(4), 690−699. https://doi.org/10.1007/s00376-020-0211-7

Ministry of Natural Resources of the People's Republic of China. (2017). China Marine Statistical Yearbook. https://cnki.nbsti.net/CSYDMirror/trade/Yearbook/Single/N2019060088?z=Z007

Monteleone, B., Borzí, I., Bonaccorso, B., & Martina, M. (2023). Quantifying crop vulnerability to weather-related extreme events and climate change through vulnerability curves. Natural Hazards, 116, 2761–2796. https://doi.org/10.1007/s11069-022-05791-0

National Bureau of Statistics of China. (2004-2019). China Statistical Yearbook. https://data.cnki.net/yearBook/single?nav=%E7%BB%9F%E8%AE%A1%E5%B9%B4%E9%89%B4&id=N2023110024

National Meteorological Information Center. (2023). Typhoon. https://data.cma.cn/article/getLeft/id/326/keyIndex/3.html [in Chinese]

Papathoma-Köhle, M., Gems, B., Sturm, M., & Fuchs, S. (2017). Matrices, curves and indicators: A review of approaches to assess physical vulnerability to debris flows. Earth-Science Reviews, 171, 272-288.

Pinelli, J.P., Pita, G., Gurley, K., Torkian, B., Hamid, S., & Subramanian, C. (2011). Damage characterization: application to Florida public hurricane loss model. *American Society of Civil Engineers*, *12*(4), 190. https://doi.org/10.1061/(ASCE)NH.1527-6996.0000051

Shifa, M., Gordon, D., Leibbrandt, M., & Zhang, M. (2022). Socioeconomic-related inequalities in COVID-19 vulnerability in South Africa. *International Journal of Environmental Research and Public Health*, *19*(17), 10480. https://doi.org/10.3390/ijerph191710480

Vamvatsikos, D., Kouris, L. A., Panagopoulos, G., Kappos, A. J., Nigro, E., Rossetto, T., ... & Stathopoulos, T. (2010). Structural vulnerability assessment under natural hazards: a review. In COST ACTION C (Vol. 26, pp. 17-18).

Vickery P.J., Lin, J., Skerlj, P.F., Twisdale, L.A., & Huang, K. (2006). HAZUS-MH hurricane model methodology I: hurricane hazard, terrain, and wind load modeling. *Natural Hazards Review*, *7*(2), 82. https://doi.org/10.1061/(ASCE)1527-6988(2006)7:2(82)

Vickery P.J., Skerlj, P.F., Lin, J., Twisdale, L.A., Young, M.A., & Lavelle F.M. (2006). HAZUS-MH hurricane model methodology II: damage and loss estimation. *Natural Hazards Review*, *7*(2), 94. https://doi.org/10.1061/(ASCE)1527-6988(2006)7:2(94)

Wan, C.C., Yan, Y.F., Shen, L.C., Liu, J.L., Lai, X.X., Qian, W., Nie, J., & Wen, J.H. (2023). Damage analysis of retired typhoons in mainland China from 2009 to 2019. *Natural Hazards*, *116*, 3225-3242. https://doi.org/10.1007/s11069-022-05804-y

Wang, S., & Toumi, R. (2021). Recent migration of tropical cyclones toward coasts. *Science*, *371*(6528), 514-+. https://doi.org/10.1126/science.abb9038

White, G.O., Boddewyn, J.J., Rajwani, T., & Hemphill, T.A. (2018). Regulator vulnerabilities to political pressures and political tie intensity: The moderating effects of regulatory and political distance. *Management International Review*, *58*, 743-769. https://doi.org/10.1007/s11575-018-0351-5

World Meteorological Organization (WMO). (2022). Tropical cyclones. https://public-old.wmo.int/en/our-mandate/focus-areas/natural-hazards-and-disaster-risk-reduction/tropical-cyclones

Xu, X.L., Sun, D.W., & Guo, T.J. (2015). A systemic analysis of typhoon risk across China, *Natural Hazards*, *77*(1), 461-477. https://doi.org/10.1007/s11069-015-1586-0

Xu, X., Qiao, S.R., Jiang, H.L., & Zhang, T. (2023). Ecosystem vulnerability to extreme climate in coastal areas of China. *Environmental Research Letters*, *18*(12), 124028. https://doi.org/10.1088/1748-9326/ad0860

Ying, M., Zhang, W., Yu, H., Lu, X., Feng, J., Fan, Y., Zhu, Y., & Chen, D. (2014). An overview of the China Meteorological Administration tropical cyclone database. *Journal of Atmospheric and Oceanic Technology*, *31*, 287-301. https://doi.org/10.1175/JTECH-D-12-00119.1

Zhang, Y., & Wang, H. (2016). A review of research on typhoon storm surge disaster risk assessment. Marine Forecasts, (02), 81-88. https://doi.org/10.11737/j.issn.1003-0239.2016.02.012

Zhong, X.C., Fang, W.H., & Cao, S.J. (2017). Probabilistic component-based Monte Carlo simulation of vulnerability for a typical low-rise rural residential building in coastal China. *Journal of Beijing Normal University (Natural Science)*, *53*(01), 51-59. https://doi.org/10.16360/j.cnki.jbnuns.2017.01.010 [in Chinese]

Zhou, Y., & Wang, J. (2012). A review on development of vulnerability curve of natural disaster. Advances in Earth Science, 27(4), 435-442.

Zhu, J.T., Liu, K., Wang, M., Xu, W., Liu, M.T., Zheng, J.C. (2022). An empirical approach for developing functions for the vulnerability of roads to tropical cyclones. *Transportation Research Part D: Transport and Environment*, *102*, 103136. https://doi.org/10.1016/j.trd.2021.103136